The exact calculation of the e. m. field arising from the scattering of twodimensional electromagnetic waves at a perfectly conducting cylindrical surface of arbitrary shape

Hoenders, B.J.

Published in:
Default journal

Publication date:
1982

Refractive index of the fly rhabdomere

D. G. M. Beersma, B. J. Hoenders, A. M. J. Huiser, and P. van Toorn

Department of Biophysics, Laboratorium voor Algemene Natuurkunde and Technisch-Fysische Laboratoria, University Groningen, Groningen, The Netherlands

Received October 1, 1979; revised manuscript received December 8, 1981

The refractive index and the diameter of the fly rhabdomere were determined by comparing the experimental results derived from interference microscopy with the results of a theoretical study on the scattering of plane waves by a homogeneous, isotropic cylindrical dielectric rod. It was found that the refractive index of the isolated rhabdomere of *Calliphora erythrocephala* is 1.363 ± 0.003 in an area of the rhabdomere where its diameter is calculated to be 1.32 ± 0.04 μm.

1. INTRODUCTION

The processing of spatial visual information by the visual system of the fly is influenced considerably by the optical properties of both the dioptrical apparatus and the photoreceptor cells. Therefore a quantitative analysis of the visual information flow requires knowledge of these optical properties, as was pointed out by Kuiper[1] and also by Seitz,[2] who studied the geometry and the refractive indices of facet lenses and pseudocones. Snyder and Pask[3] emphasized that the study of the optical parameters should include the waveguide properties of the rhabdomere, i.e., the visual pigment containing rodlike part of the visual sensory cells. The important parameters here are the diameter of the rhabdomere and the refractive indices of the rhabdomere and its surroundings; these parameters determine the fraction of the incident light power propagated within the rhabdomere's boundary and also the rhabdomere's acceptance angle.[4,5]

On the strength of these implications of the waveguide properties for visual processing, Kirschfeld and Snyder[6,7] suggested various methods to determine the refractive index of the rhabdomere; however, no accurate values have been obtained thus far.

In the present study, a newly developed direct method is presented by which it is possible to determine accurately both the value of the refractive index and the diameter of isolated rhabdomeres suspended in physiological saline. Essentially, the rhabdomere is regarded as a cylindrical dielectric rod, and the scattering of plane waves by this rod is studied by interference microscopy.

A large body of literature exists devoted to the determination of the refractive indices of optical fibers by using the Born or the Glauber approximation.[8–11] The magnitude of the error inherent in these approximations is not *a priori* clear for the rhabdomere considered in our study. As a consequence, we decided to deal with a numerical approach to the exact solution of the scattering problem.

2. MATERIALS AND METHODS

The refractive-index measurements were performed on squash preparations of rhabdomeres from the eyes of the white-eyed blowfly mutant Chalky (*Calliphora erythrocephala* M.).

A. Preparation

After decapitation of the fly, the retina was carefully separated from the optic ganglia and subsequently submerged in an insect Ringer solution where it was fractioned with a razor blade. The resulting suspension was then covered with a cover slip, squashed, and viewed through an interference microscope (Zeiss microscope equipped with Jamin–Lebedeff interference optics). This preparation technique frequently yielded isolated ommatidia with the retinular cells partly broken down. Occasionally, however, ommatidia were found in which one or more of their rhabdomeres were curving away from the others (Fig. 1), which were used for the measurements.

B. Experimental Procedure

Under monochromatic illumination, objects with different refractive-index values become apparent as such when viewed through an interference microscope. Such objects can be distinguished from objects with different absorption properties by variation of the phase difference δ between the two interfering beams. One must realize that the brightness of a homogeneous object of constant thickness depends sinusoidally on δ. When structures in addition have identical refractive-index values, they have their brightness maxima at

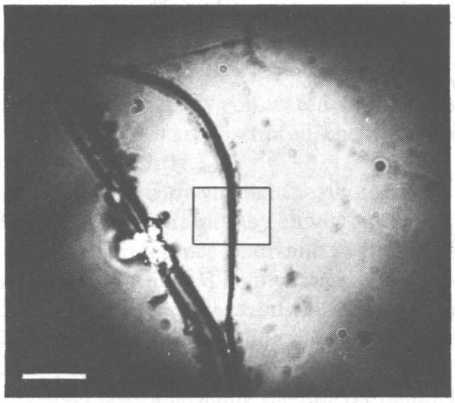

Fig. 1. Bundle of rhabdomeres suspended in insect Ringer solution as seen in interference microscopy. Notice that one rhabdomere is partly isolated. The experiments are performed on isolated rhabdomeres such as this one. The horizontal bar represents 10 μm. The rectangle marks the part of the rhabdomere that is studied in Fig. 2.

0030-3941/82/050583-06$01.00

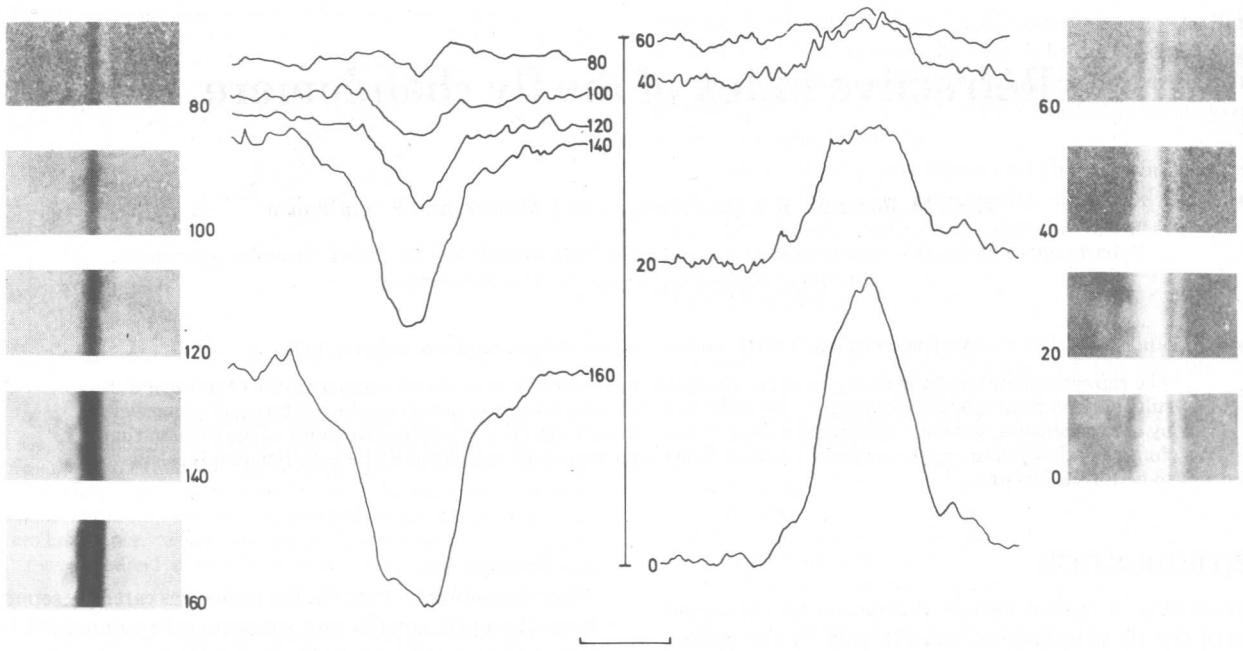

Fig. 2. Isolated rhabdomeres photographed at different relative phase values δ between the interfering beams in the microscope. These photographs are positives; the negatives were scanned with a densitometer, yielding the above curves. The numbers in the figure denote δ values. The horizontal bar represents 1 μm; the vertical bar represents 1-log-unit density.

identical values of δ. However, objects differing in refractive index have their sinusoidal brightness modulations displaced along the δ axis; this displacement depends on both the magnitude of the difference in refractive index and the thickness of the object.

In the actual experiment performed at $\lambda = 546$ nm, δ was varied in steps of 20°, and the interference pattern was photographed after each step with a constant exposure time. The negatives were scanned with a densitometer along a line perpendicular to the rhabdomere (Fig. 2). Thus, for each point along that same pathway in the preparation, nine (180°/20°) density values were obtained, or one density value from each photograph. In Fig. 3, these values are plotted as functions of δ for two important locations in the preparation: a cross indicates a point on the axis of the rhabdomere, and a circle indicates a point located in the clear Ringer solution. (The curves deviate from a sine function because of the nonlinear transfer characteristics of the photographic emulsion.)

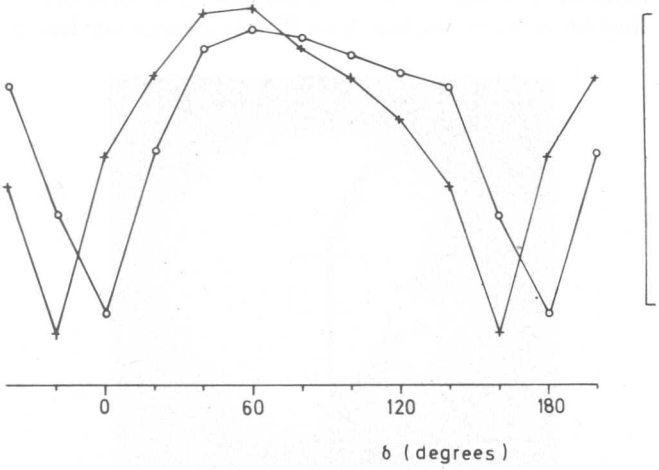

Fig. 3. Density values at appropriate locations taken from the curves of Fig. 2 and plotted as functions of δ. The circles are obtained for points located in clear Ringer solution. The crosses denote measurements obtained at the centers of the rhabdomeres. The mutual shift of the two curves is called σ and is obtained by a cross-correlation procedure.

From such pairs of curves the relative displacements σ along the δ axis were determined by a cross-correlation procedure, yielding the phase differences between the incident plane wave and the scattered wave. For this purpose, the curves of Fig. 3 are sampled at 1° intervals by linear interpolation. From the σ values the refractive-index difference between the isolated rhabdomere and the surrounding Ringer solution was calculated.

C. Theoretical Approach

Because the rhabdomere's diameter is of the order of the wavelength of the applied illumination, geometrical optics cannot be used to calculate the refractive index of a rhabdomere. Therefore, scattering of electromagnetic waves by a dielectric cylinder is studied. Solving Maxwell's equations leads to the series expansions (in polar coordinates)

$$H_z(\rho, \phi) = \sum_m (-i)^m [J_m(k\rho) + b_m H_m^{(1)}(k\rho)] \exp(im\phi),$$

$$\rho \geqq a, \qquad \mathbf{H} \parallel Z \text{ axis},$$

$$b_m = \frac{J_m(ka)J_m'(nka) - nJ_m'(ka)J_m(nka)}{nJ_m(nka)H_m'^{(1)}(ka) - J_m'(nka)H_m^{(1)}(ka)}$$

or

$$E_z(\rho, \phi) = \sum_m (-i)^m [J_m(k\rho) + c_m H_m^{(1)}(k\rho)] \exp(im\phi),$$

$$\rho \geqq a, \qquad \mathbf{E} \parallel Z \text{ axis},$$

$$c_m = \frac{nJ_m(ka)J_m'(nka) - J_m'(ka)J_m(nka)}{J_m(nka)H_m'^{(1)}(ka) - nJ_m'(nka)H_m^{(1)}(ka)}$$

(see Ref. 12).

With these equations it is possible to calculate the phase shift σ and the intensity of the scattered wave at any position $\rho \neq 0$ in the field and for any combination of the input parameters n and d (n represents the refractive-index ratio of the rhabdomere and the Ringer solution; d equals twice the radius a of the rhabdomere).

The statement that the series expansions for the field components hold for $\rho \neq 0$ is proven as follows:

Recalling that for arbitrary complex values of x

$$J_m(x) = 0\left(\frac{x^m}{m!2^m}\right)$$

and

$$H_m(x) = 0\left[\frac{2^{m+1}(m-1)!}{x^{m+1}}\right]$$

(see Ref. 13, lemmas 27 and 30), we observe that

$$b_m = 0\left[\frac{1}{(m!)^2}\right]$$

and

$$c_m = 0\left[\frac{1}{(m!)^2}\right].$$

This implies that the series expansion describing H_z (and the expansion describing E_z) is uniformly convergent in any bounded domain of the complex ρ, ϕ space, excluding $\rho = 0$. According to the Weierstrass theorem (see Ref. 14), this means that the series expansion is analytic for $\rho \neq 0$. The field in the image space of the microscope is analytic also (Ref. 13, lemma 48). This field is represented by the series expansion depicted above for $|\rho| \geqq a$. The analyticity of both the field and the series expansion guarantees that the series expansion holds for $0 < |\rho| \leqq a$.

D. Fitting Procedure

An iterative procedure has yielded the desired values of the parameters n and d. First the values of n and d were arbitrarily chosen, and the phase-shift profile was calculated. Height and width at half-height of this curve were compared with the same dimensions of the experimental profile (see Fig. 4). In the geometrical-optical limit, the height of the curve is proportional to d. Although the theory of geometrical optics is not valid in the present situation, it enables one to approach quickly the values of the parameters that determine the best-fitting curve. The inaccuracies of the parameters were numerically evaluated in the same way by accounting for the standard errors of the experimental data: the smallest possible half-width of the experimental curve is combined with the maximum possible height, and the parameters n and d are evaluated to fit the curve. Additionally, the maximum half-width is combined with the minimum height to find the other limits of the parameters.

3. RESULTS

The refractive index of the isolated fly rhabdomere was determined by interference microscopy. Since it is difficult to distinguish between fractioned isolated rhabdomeres and other particles in the solution, only rhabdomeres curving away from the ommatidium were examined. Figure 1 is a photograph of such a preparation. Since preparations like the one shown are not encountered frequently, it may be assumed that the rhabdomeres are tightly connected. (Even when the retinular cell membranes are disrupted, the rhabdomeres usually cling together tightly.)

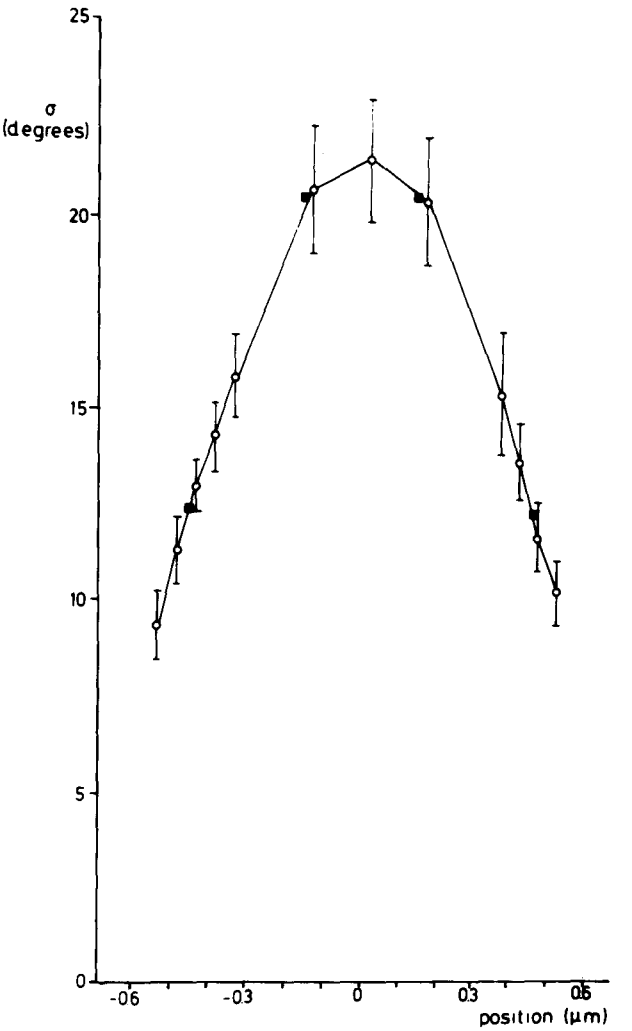

Fig. 4. In seven rhabdomeres, all at a distance of approximately 100 μm from the distal tips, σ values were obtained as functions of the distance between the measurement location and the center of the rhabdomere. The mean values of σ (circles) and the standard errors (bars) are plotted. The filled squares are σ values obtained by running the computer program on scattering of plane waves by a cylinder, assuming that the ratio of the refractive indices of the cylinder and the surrounding medium is 1.018 and that the diameter of the cylinder is 1.32 μm.

Interference microscopy yielded the photographs presented in Fig. 2, which were obtained by changing the phase difference δ between the reference beam and the beam transmitted through the preparation. The illumination wavelength was 546 nm. The density profiles resulting from scanning across the negatives along a straight line perpendicular to the axis of the rhabdomere are also shown in Fig. 2. A sample of accurately defined positions along the line perpendicular to the rhabdomere, i.e., the horizontal axis in Fig. 2, was selected. For each of these positions, the corresponding nine density values were taken from the curves and plotted as functions of δ. Plots such as these were compared with the plot that was obtained at a clear location in the Ringer solution (Fig. 3).

Measurements of the phase differences σ were performed on seven isolated rhabdomeres. All measurement locations were approximately halfway along the length of the rhabdomeres. The mean values of σ as a function of the position along the line of scanning (perpendicular to the rhabdomere) are presented in Fig. 4. The filled squares in this figure represent σ values derived theoretically (see Section 2.C). The parameter values needed to describe the experimental results are

$$n = 1.018 \pm 0.002\ \mu\text{m},$$

$$d = 1.32 \pm 0.04\ \mu\text{m}.$$

Since n is defined as the ratio between the refractive index of the rhabdomere and the insect Ringer solution (which refractive index was determined with the aid of a refractometer to be 1.3352), we arrive at

$$n_{\text{rhabdomere}} - n_{\text{Ringer}} = 0.024 \pm 0.003.$$

Hence the refractive index of the rhabdomere while suspended in the insect Ringer solution is 1.359 ± 0.003. If the difference in refractive index between the rhabdomere and the surrounding medium in tissue is the same as the difference in refractive index between the rhabdomere and the Ringer solution, then

$$n_{\text{rhabdomere}} = 1.363 \pm 0.003 \text{ (at } \lambda = 546 \text{ nm}).$$

Here the refractive index of the medium surrounding the rhabdomere in tissue is taken to be 1.339 (see below).

4. DISCUSSION

A. Comparison of Experimental and Theoretical Results

The refractive index of the fly rhabdomere at 546 nm was determined to be 1.363 ± 0.003 by comparison of the results derived from an experimental and a theoretical study. Some details of the procedure need further discussion.

In the theoretical approach, the scattering of plane waves by a cylinder is considered. In the experimental arrangement, plane-wave illumination can be approximated only at the expense of intensity, leading to long exposure times during which the preparation deteriorates. Therefore an incident beam of light having an aperture half-width value of 6° was applied, and, in calculating the profiles, this wider aperture should be accounted for. However, this (computer-) time-consuming approach can be avoided experimentally by focusing the microscope at the axis of the rhabdomere where the least amount of fading of the image because of the finite aperture of the illumination occurs. Yet a second problem is created by this focusing method: the comparison of theory and experiment demands calculations of σ near the axis of the rhabdomere, and in that region the series expansions for the fields do not converge sufficiently fast. A satisfactory solution was obtained by estimating the phase differences σ in locations at a distance of less than 0.5 μm from the axis of the rhabdomere in the plane perpendicular to the direction of the incident-wave propagation by interpolating the results obtained along the line of the incident-wave propagation.

The reliability of this interpolation is best at the locations indicated in Fig. 4. This can be seen from Fig. 5, in which two σ curves are plotted. The single-peaked curve is an estimation of the σ curve as it will be found 1 μm above or below the axis of the rhabdomere. The double-peaked curve is an estimation of the σ curve as it will be found in the plane through the axis of the rhabdomere along a line perpendicular to the axis.

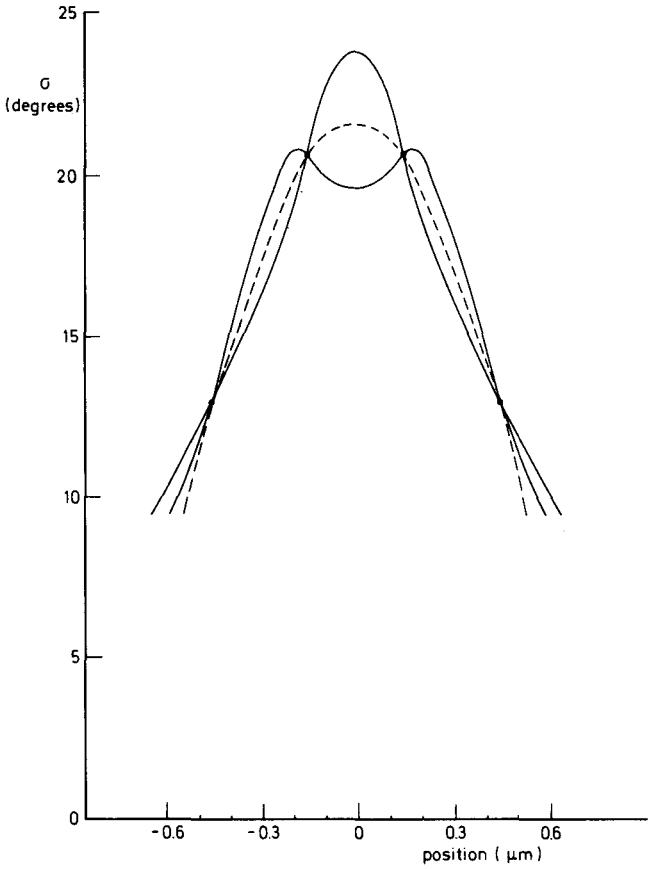

Fig. 5. Theoretical dependence of σ on the position along a line perpendicular to the axis of the rhabdomere. The double-peaked curve is found when a microscope with zero focal depth is focused at the axis of the rhabdomere. The single-peaked curve results when the microscope is focused 1 μm above or below the center of the rhabdomere.

Obviously the shape of the σ curve depends strongly on the focusing of the microscope and therefore also on the focal depth of the microscope. However, there are two locations in the field at both sides of the axis of the rhabdomere where σ is almost independent of focusing in a range of several micrometers. These are the points in Fig. 5 where the two curves intersect. From Fig. 5 it thus can be seen that the precise shape of the experimental curve of Fig. 4 is not easily predicted. (As a matter of fact, the shape of the curve lies between the two curves of Fig. 5.) However, since the σ values at the marked locations are almost independent of focusing of the microscope, these values are much more reliable.

Theoretically, the phase differences σ are only slightly influenced by the orientation of the plane of polarization of the incident light. Both in the calculations leading to Fig. 5 and in the experiments, the plane of polarization of the incident light and the axis of the rhabdomere enclosed an angle of 45°.

B. Diameter of the Rhabdomere

The mean value of the diameters of seven rhabdomeres at a distance of approximately 100 μm from the distal tips (the

total length of the rhabdomere is about 200 μm) was determined to be 1.32 ± 0.04 μm. It is most likely that the data obtained apply only to the six peripheral rhabdomeres. Within the fly ommatidium there are two types of rhabdomeric cylinder,[15,16] one central cylinder having a constant diameter and six peripherally located tapering rhabdomeres. In the present study, it is likely that only the latter population was encountered because of the apparent mutual adherence of the rhabdomeres.

The value of 1.32 μm for the diameter of the rhabdomere correlates well with the data obtained by using the electron microscope. According to Horridge *et al.*,[16] the rhabdomere diameter in *Calliphora stygia* near the distal tips is approximately 1.8 μm. In *Musca*, the diameter of the peripheral rhabdomere decreases along its length almost linearly by about a factor of 2.[15] Assuming that the observed decrease of the rhabdomere's diameter in *Calliphora* behaves accordingly, a rhabdomere diameter value of 1.35 μm at 100 μm from the distal tips is expected. This value approximates closely the one derived above.

C. Refractive Index of the Rhabdomere

Birefringence

The ultrastructure of the rhabdomere is known from studies performed using an electron microscope (see, e.g., Ref. 15). The rhabdomere consists of microvilli oriented perpendicularly to the axis of the rhabdomere and aligned in parallel. This anisotropy can cause birefringence, as was argued by Israëlachvilli *et al.*[17]

However, it was concluded from these investigations that the difference in refractive index for light polarized parallel or perpendicularly to the microvilli amounts to less than 0.001. Since the experimental inaccuracy in determining refractive-index values of rhabdomeres exceeds this figure by a factor of 3, the birefringence is not resolved by this method.

Refractive Index in Tissue

The refractive index of the rhabdomere in tissue is calculated as follows: According to Israëlachvilli *et al.*,[17] the rhabdomere in tissue consists of three distinct volume fractions. Approximately 60% of the rhabdomere is intracellular cytoplasm, the refractive index of which was determined by Seitz[2] to be 1.341. About 30% of the rhabdomere consists of cell membrane, and the remaining 10% is extracellular liquid with a refractive index of 1.336, according to the measurements of Seitz. Assuming that a complete exchange of liquids occurs in the preparation (see Ref. 6), the rhabdomere's refractive index in tissue is found by adding two correction terms to the refractive-index value as it was obtained in the Ringer solution (1.359). The first correction term concerns the influence of the 60% cytoplasm volume fraction. The magnitude of this correction is $0.6 \times (1.341 - 1.3352) = 0.0036$. The second term corrects for the influence of the extracellular liquid and is $0.1 \times (1.336 - 1.3352) = 0.0001$. Hence the refractive index of the rhabdomere in tissue (n_1) is calculated to be 1.363.

Another important parameter for the description of the wave propagation of light through the rhabdomere is the refractive index of the medium surrounding the rhabdomere, called n_2. The value 1.339 was taken as the mean of the refractive indices of the cytoplasm and the extracellular liquid (see above).

The refractive-index values of the rhabdomere (n_1) and the surrounding medium (n_2), together with the diameter of the rhabdomere and the wavelength of the applied illumination, determine the waveguide parameter V, defined as follows:

$$V = \frac{\pi d}{\lambda}(n_1^2 - n_2^2)^{1/2}.$$

The data shown in this paper indicate that $V = 1.9 \pm 0.2$ at a distance of 100 μm from the distal tips of the rhabdomeres. Extrapolating these results to the distal tips of the rhabdomeres, it is found (with $d = 1.8$ μm) that $V = 2.6 \pm 0.3$. This value can be compared with the findings of Kirschfeld and Snyder,[6,7] who determined the effective value of V in the distal part of a rhabdomere by studying the birefringence of the rhabdomeres at different wavelengths. They arrived at $V = 2.8 \pm 0.6$ at 546 nm on the basis of several assumptions. A major uncertainty in their work concerns the diameters of those rhabdomeres that were studied. However, despite the question of whether the different results can be reliably compared, obviously the agreement is reasonable.

D. Implications of the Obtained Refractive-Index Value

Stavenga[18] determined the refractive index of the fly rhabdomere by correcting the results of Seitz[2] for waveguide effects. Both the correction method of Stavenga and the measurement technique of Seitz were questioned by Kirschfeld and Snyder.[6] Nevertheless, the refractive-index value of the rhabdomere estimated by Stavenga (1.365 ± 0.006) is confirmed by the present study. Therefore the extensive discussions of Stavenga[19] on the implications of the refractive-index value in other studies are reinforced by the present findings.

The refractive index of the rhabdomere, together with the refractive index of its surroundings, the rhabdomere's diameter, and the wavelength of the applied illumination, determines the acceptance angle of the rhabdomere. At $\lambda = 546$ nm the acceptance angle of the rhabdomere amounts to 16° (calculated from Ref. 5). This acceptance angle seems to be slightly smaller than the aperture of the cone in the fly ommatidium, which can be calculated from the results of Stavenga[20] in the case of *Musca*. Assuming that *Calliphora* and *Musca* have about the same cone aperture, the rhabdomere acceptance angle of 16° should be compared with a cone aperture of 20°. Hence the acceptance angle of the rhabdomere is sufficiently large to collect a large fraction of the incident light power.

Another important aspect of the wave propagation of light through a rhabdomere is the fraction of the light power that is guided outside the rhabdomere's boundary. This fraction is of functional importance because of the existence of the so-called intracellular pupil mechanism. Granules inside the photoreceptor cells migrate on light adaptation toward the rhabdomere and regulate, by absorption and scattering of the boundary wave, the light flux through the rhabdomere.[21,22] It is easily estimated (see Ref. 5) that the fraction of the incident light power propagating outside the boundary of the rhabdomere amounts to approximately 15%.

ACKNOWLEDGMENTS

We thank D. G. Stavenga and J. Tinbergen for many constructive discussions. We are grateful to J. T. Leutscher-Hazelhoff for correcting the manuscript.

REFERENCES

1. J. W. Kuiper, "On the image formation in a single ommatidium of the compound eye in Diptera," in *The Functional Organization of the Compound Eye*, C. G. Bernhard, ed. (Pergamon, Oxford, 1966), pp. 35–50.
2. G. Seitz, "Der Strahlengang im Appositionsauge von *Calliphora erythrocephala* (Meig)," Z. Vergl. Physiol. **59,** 205–231 (1968).
3. A. W. Snyder and C. Pask, "Spectral sensitivity of dipteran retinula cells," J. Comp. Physiol. **84,**59–76 (1973).
4. A. W. Snyder, "Excitation and scattering of modes on a dielectric or optical fiber," IEEE Trans. Microwave Theory Tech. **MTT-17,** 1138–1144 (1969).
5. A. W. Snyder, "Optical properties of invertebrate photoreceptors," in *The Compound Eye and Vision of Insects*, G. A. Horridge, ed. (Clarendon, Oxford, 1975), pp. 179–235.
6. G. K. Kirschfeld and A. W. Snyder, "Waveguide mode effects, birefringence and dichroism of fly receptors," in *Photoreceptor Optics*, A. W. Snyder and R. Menzel, eds. (Springer-Verlag, Berlin, 1975), pp. 56–77.
7. K. Kirschfeld and A. W. Snyder, "Measurements of a photoreceptor's characteristic waveguide parameter," Vision Res. **16,** 775–778 (1976).
8. L. S. Watkins, "Scattering from side-illuminated clad glass fibers for determination of fiber parameters," J. Opt. Soc. Am. **64,** 767–772 (1974)
9. T. Okoshi and K. Hotate, "Refractive index profile of an optical fiber: its measurement by the scattering-pattern method," Appl. Opt. **15** 2756–2764 (1976).
10. E. Brinkmeyer, "Refractive index profile determination of optical fibers from the diffraction pattern," Appl. Opt. **16,** 2802–2803 (1977).
11. P. L. Chu and T. Whitbread, "Non-destructive determination of refractive index profile of an optical fiber: fast Fourier transform method," Appl. Opt. **18,** 1117–1122 (1979).
12. J. R. Wait, *Electromagnetic Radiation from Cylindrical Structures* (Pergamon, New York, 1959), pp. 142–146.
13. C. Müller, "Foundations in the mathematical theory of electromagnetic waves," in *Die Grundlehren der mathematischen Wissenschaften in Einzeldarstellungen* (Springer-Verlag, Berlin, 1969), Band 155.
14. W. F. Osgood, *Lehrbuch der Funktionentheorie II*, (Teubner, Berlin, 1929), Vol. 1, Sec. 1.8, p. 15,
15. C. B. Boschek, "On the fine structure of the peripheral retina and lamina ganglionaris of the fly, *Musca domestica*," Z. Zellforsch. Mikrosk. Anat. **118,** 369–409 (1971).
16. G. A. Horridge, K. Mimura, and R. C. Hardie, "Fly photoreceptors. III. Angular sensitivity as a function of wavelength and the limits of resolution," Proc. R. Soc. Lond. Ser. B **194,** 151–177 (1976).
17. J. N. Israëlachvilli, R. A. Sammut, and A. W. Snyder, "Birefringence and dichroism of photoreceptors," Vision Res. **16,** 47–52 (1976).
18. D. G. Stavenga, "Refractive index of fly rhabdomeres," J. Comp. Physiol. **91,** 417–426 (1974).
19. D. G. Stavenga, "Waveguide modes and refractive index in photoreceptors of invertebrates," Vision Res. **15,** 323–330 (1975).
20. D. G. Stavenga, "Optical qualities of the fly eye. An approach from the side of geometrical, physical and waveguide optics," in *Photoreceptors Optics*, A. W. Snyder and R. Menzel, eds. (Springer-Verlag, Berlin, 1975, pp. 126–144.
21. K. Kirschfeld and N. Franceschini, "Ein Mechanismus zur Steuerung des Lichtflusses in den Rhabdomeren des Kmplexauges von *Musca*," Kybernetik **6,** 13–22 (1969).
22. N. Franceschini and K. Kirschfeld, "Le contrôle automatique du flux lumineux dans l'oeil composé des diptères. Propriétés spectrales, statiques et dynamiques du mécanisme," Biol. Cybernetics, **21,** 181–203 (1976).